International Journal of Applied Engineering Research
ISSN 0973-4562 Volume 10, Number 6 (2015) pp. 14431-14448

http://www.ripublication.com

Reference Current Generation For Shunt Active Filter Using Various Algorithms

P.Arthi1, R.Sriranjani2, M.Balasubramani3

1,2,3 Department of Electrical and Electronics Engineering, SASTRA University
Thanjavur - 613 401, Tamilnadu, India
arthipanneer@gmail.com

Abstract

In recent times, the introduction of harmonics due to the presence of Non-linear loads affects the power quality in distribution systems. The objective of this paper is to improve the power quality by using a shunt active power filter (SAPF), to reduce the current harmonics injected in the source side from the load side. In this paper, voltage source inverter (VSI) acts as a filter which is connected parallel to the load through a reactor which is fused. Shunt active power filter eliminates the harmonics by intruding harmonic current into the line with equal magnitude and different phase to that of load current harmonics. SAPF using different control strategies such as Instantaneous Real and Reactive Power (IRP) theory, Synchronous Reference Frame (SRF) theory, Current Source (CS) Scheme and Power balance (PB) Scheme are introduced for harmonic mitigation, with same load conditions and different current controllers. When a nonlinear load is connected to the system, harmonics gets introduced in the supply side due to the nonlinearity. Therefore, it is necessary to minimize the Total Harmonic Distortion (THD) of the source current. Based on the minimization of source current THD, the performance of different control strategies with different controllers is related and the results of simulation are examined using the SIMULINK model.
Index Terms: Shunt Active Power Filter, Active Power Filter, Voltage Source Inverter, Instantaneous Real and Reactive Power, Synchronous Reference Frame, Current-Source, Power-Balance, Total Harmonic Distortion.

Introduction

Due to the usage of nonlinear loads, the effect of harmonics [1] in power system distributions is becoming more severe nowadays. The harmonics due to Non-Linear load causes power loss in power system components, which in turn results in

increased heat liberation in the power system components. In addition to this, the self lifetime of the components also gets reduced. To overcome this problem, filters are chosen to cancel out the current harmonics.

When a load which is non-linear is connected to the system, the current waveform will not follow the supply voltage. The current waveform will be distorted and contains current harmonics in it. The presence of current harmonics in a system can be determined by the presence of high neutral current, compared to the currents in the three phases [2]. The current harmonics are the main cause for the voltage distortions. Therefore, the main aim is to reduce the current harmonics, which in turn reduces the voltage distortions and makes the system less prone to harmonics. The total harmonic distortion of a current waveform is given by,

$$THD_{Ir}=\frac{1}{I_{1r(rms)}}\sqrt{\left(\sum_{h=2}^{\infty}I_{hr(rms)}^{2}\right)} \quad (1)$$

Where, I_{1r} is the fundamental current and I_{hr} is the harmonic current.

The extent to which the waveform of the voltage gets distorted is given by,

$$THD_{vr}=\frac{1}{V_{1r(rms)}}\sqrt{\left(\sum_{h=2}^{\infty}V_{hr(rms)}^{2}\right)} \quad (2)$$

Where, V_1 is the fundamental voltage and V_h is the harmonic voltage. Zero-crossing noise and voltage distortion in induction motors are the problems caused by voltage harmonics.

In earlier days, the main sources of harmonics were considered to be transformers and rotating machines, since they operate the magnetic materials in the nonlinear region for economic purposes. Later on, after power semiconductor devices [3] were introduced, it was found that the sources of harmonics were mainly from power electronic devices. One of the sources of harmonics is SMPS, which is found in most of the electronic devices.

Systems with unity power factor are efficient systems. The true power factor is given by,

$$pf_{true1} = dpf_{11}*pf_{dist1} \quad (3)$$

Where, Pf_{true} is the true power factor, dpf_1 is the displacement power factor, pf_{dist} is the distortion power factor. True power factor is considered for non-linear loads. For linear loads, they are equal. Power factor [4] gets reduced because of the distortions caused due to harmonics.

Three types of filters that are used to eliminate harmonics [5] are Active filters, Passive filters and Hybrid filters [6],[7]. Compared to passive filters, active filters [8] have good flexibility, less cost and better filtering performance. Classifications of APF are series APF, shunt APF and hybrid APF. Since the cancellation of current harmonics is considered, shunt active power filter is used. Cancelling of load current harmonics injected into the supply is the main purpose of the filter. The control techniques used are IRP theory [9]-[12], SRF theory, CS and PB schemes. Current controllers used are Hysteresis controller [13], PWM controller and VR controller

[14]. The control techniques and the current controller proposed in this paper are Current Source (CS) scheme, Power Balance (PB) scheme and Vector Resonant (VR) controller. Among different control techniques [15], basic control techniques namely IRP and SRF are used because of its simplicity and easy calculations. VR controller is choosen because of the excellent selectivity it has for eliminating the harmonic frequency.

Control Techniques

Control techniques are used for the generation of reference filter current or reference source current. For the propagation of reference filter current IRP theory is applied and for the propagation of reference source current SRF theory is applied.

A. Instantaneous real and reactive power theory (p-q theory)

Since, IRP theory is based on time domain, they can operate both in steady-state and transient-state conditions. Even though, there are many methods available for harmonic detection, only p-q theory and SRF theory is popular because of their best results. IRP theory allows the control of APF in real time. The advantage of this theory is its simple calculations. The three phase voltages are denoted as $V_{ar,}$ V_{br} and V_{cr} and the three phase line currents are denoted as $i_{ar,}$ $i_{br,}$ i_{cr}. They are transformed into $\alpha\beta o$ co-ordinates, which are known as Clarke's transformation. The transformations are as follows,

$$i_{\alpha r}=\frac{\sqrt{2}}{\sqrt{3}}i_{ar}-\frac{1}{\sqrt{6}}i_{br}-\frac{1}{\sqrt{6}}i_{cr} \tag{4}$$

$$i_{or}=\frac{1}{\sqrt{3}}i_{ar}+\frac{1}{\sqrt{3}}i_{br}+\frac{1}{\sqrt{3}}i_{cr} \tag{5}$$

$$i_{\beta r}=\frac{1}{\sqrt{2}}i_{br}-\frac{1}{\sqrt{2}}i_{cr} \tag{6}$$

$$V_{0r}=\frac{1}{\sqrt{3}}V_{ar}+\frac{1}{\sqrt{3}}V_{br}+\frac{1}{\sqrt{3}}V_{cr} \tag{7}$$

$$V_{\alpha r}=\frac{\sqrt{2}}{\sqrt{3}}V_{ar}-\frac{1}{\sqrt{6}}V_{br}-\frac{1}{\sqrt{6}}V_{cr} \tag{8}$$

$$V_{\beta r}=\frac{1}{\sqrt{2}}V_{br}-\frac{1}{\sqrt{2}}V_{cr} \tag{9}$$

The three instantaneous powers calculated from load side are,

$$p_{or\_load}=v_{or}i_{or} \tag{10}$$

$$p_{\alpha\beta r\_load}=v_{\alpha r}i_{\alpha r}+v_{\beta r}i_{\beta r} \tag{11}$$

$$q_{\alpha\beta r\_load}=v_{\alpha r}i_{\beta r}-v_{\beta r}i_{\alpha r} \tag{12}$$

The reference compensating instantaneous powers is,

$$p_{0r}^{*}=-p_{0r}\_load \tag{13}$$

$$p_{\alpha\beta r}^{*}=-p_{\alpha\beta r\_load\_ac} \tag{14}$$

Where,

$p_{\alpha\beta r\_load\_ac}$ is the AC part of $p_{\alpha\beta r\_load}$

$$q_{\alpha\beta r}^{*}=-q_{\alpha\beta r\_load} \tag{15}$$

The compensating currents in the α-β-o co-ordinates calculated from the reference compensating instantaneous powers are,

$$i_{cor}=\frac{p_{0r}^{*}}{v_{0r}}-i_{0r} \tag{16}$$

$$i_{c\alpha r}=\left(\frac{v_{\alpha r}}{v_{\alpha\beta r}^{2}}\right)p_{\alpha\beta r}^{*}+\left(\frac{-v_{\beta r}}{v_{\alpha\beta r}^{2}}\right)q_{\alpha\beta r}^{*} \tag{17}$$

$$i_{c\beta r}=\left(\frac{v_{\beta r}}{v_{\alpha\beta r}^{2}}\right)p_{\alpha\beta r}^{*}+\left(\frac{v_{\alpha r}}{v_{\alpha\beta r}^{2}}\right)q_{\alpha\beta r}^{*} \tag{18}$$

Where,

$v_{\alpha\beta r}=v_{\alpha r}^{2}+v_{\beta r}^{2}$

The compensating currents in the a-b-c coordinates are,

$$i_{car}=0.57i_{c0r}+0.82i_{c\alpha r} \tag{19}$$

$$i_{cbr}=0.57i_{c0r}-0.41i_{c\alpha r}+0.707i_{c\beta r} \tag{20}$$

$$i_{ccr}=0.577i_{c0r}-0.41i_{c\alpha r}-0.707i_{c\beta r} \tag{21}$$

B. Synchronous Reference Frame Theory (SRF theory)

Another conventional strategy used for reference current generation is the Synchronous reference frame. The analysis of three phase circuits can be simplified by a mathematical transformation named direct-quadrature. They are transformed back to original three phase AC quantities from the two phase DC quantities in terms of current. These transformations are applicable only for balanced three phase circuits. The three phase line current and three phase voltage equations transformed into α-β-o coordinates are as follows,

$$i_{\alpha r}=\frac{\sqrt{2}}{\sqrt{3}}i_{ar}-\frac{1}{\sqrt{6}}i_{br}-\frac{1}{\sqrt{6}}i_{cr} \tag{22}$$

$$i_{or}=\frac{1}{\sqrt{3}}i_{ar}+\frac{1}{\sqrt{3}}i_{br}+\frac{1}{\sqrt{3}}i_{cr} \tag{23}$$

$$i_{\beta r}=\frac{1}{\sqrt{2}}i_{br}-\frac{1}{\sqrt{2}}i_{cr} \tag{24}$$

$$V_{0r}=\frac{1}{\sqrt{3}}V_{ar}+\frac{1}{\sqrt{3}}V_{br}+\frac{1}{\sqrt{3}}V_{cr} \tag{25}$$

$$V_{\alpha r}=\frac{\sqrt{2}}{\sqrt{3}}V_{ar}-\frac{1}{\sqrt{6}}V_{br}-\frac{1}{\sqrt{6}}V_{cr} \tag{26}$$

$$V_{\beta r}=\frac{1}{\sqrt{2}}V_{br}-\frac{1}{\sqrt{2}}V_{cr} \tag{27}$$

$\theta_r=\tan^{-1}\frac{V_{\beta r}}{V_{\alpha r}}$, Where θ_r is the angle between α and β

$$\text{(i.e.) } \theta_r=\tan^{-1}\left[\frac{\left(\frac{1}{\sqrt{2}}V_{br}-\frac{1}{\sqrt{2}}V_{cr}\right)}{\left(\frac{\sqrt{2}}{\sqrt{3}}V_{ar}-\frac{1}{\sqrt{6}}V_{br}-\frac{1}{\sqrt{6}}V_{cr}\right)}\right] \tag{28}$$

The current equations in d-q coordinates are,

$$i_{dr}=\cos\theta_r i_{\alpha r}+\sin\theta_r i_{\beta r} \tag{29}$$

$$i_{qr}=-\sin\theta_r i_{\alpha r}+\cos\theta_r i_{\beta r} \tag{30}$$

Three phase compensated reference current calculated by inverse park transform is,

$$i_{carref}=i_{dr}\sin(\omega t)+i_{qr}\cos(\omega t) \tag{31}$$

$$i_{cbrref}=i_{dr}\sin\left(\omega t-\frac{2\pi}{3}\right)+i_{qr}\cos\left(\omega t-\frac{2\pi}{3}\right) \tag{32}$$

$$i_{ccrref}=i_{dr}\sin\left(\omega t+\frac{2\pi}{3}\right)+i_{qr}\cos\left(\omega t+\frac{2\pi}{3}\right) \tag{33}$$

Where, $\omega=2\pi f$ and f=50Hz

C. Current Source Scheme (CS)

Two types of current detection are load current detection and source current detection. The classifications of Source current detection are Current Source Scheme and Power balance scheme. Block diagram of CS scheme is shown in Fig.1. Here, the control

target is the source current, since the non-linearity is intruded in the supply side of the nonlinear load.

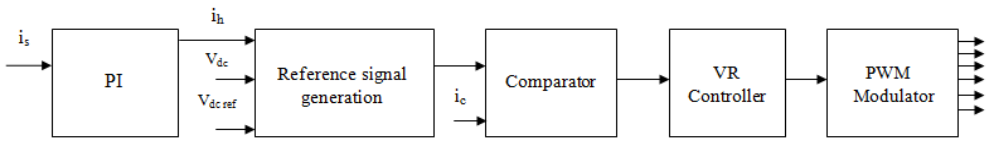

Figure 1: Block diagram of current source scheme

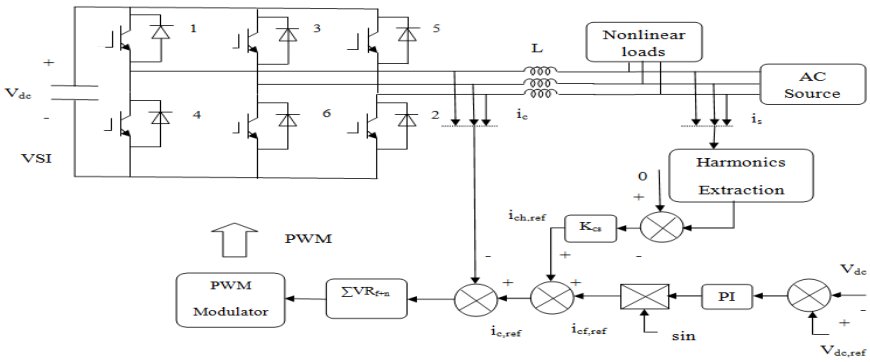

Figure 2: Schematic of current source scheme

Schematic of this scheme is shown in Fig.2. In the current source scheme, p-q theory is used for harmonic extraction. The filtering performance of the shunt APF is determined by the gain k_{cs}. By comparing the voltage of a DC capacitor with its reference value and applying its error to the PI controller, compensation of inverter power loss and maintenance of DC voltage within the desired limit is achieved.

The difference of voltage of capacitor which is DC and its reference is given to the PI controller. The output of PI controller when multiplied with sinθ gives the fundamental reference of the compensating current. The harmonic current extracted by the p-q theory is multiplied with the proportional term $k_{cs,}$ to give harmonic reference of the compensating current. Addition of fundamental reference of the compensating current and the harmonic reference of the compensating current gives the reference signal.

D. Power Balance Scheme (PB)

Block diagram of PB scheme is shown in Fig.3. The power balance scheme has good filtering performance under stable condition. Under unstable conditions the regulation of V_{dc} is affected. To minimize the fluctuation of the V_{dc}, DC capacitor of larger size

is required. The computations involved in this scheme are reduced, since the harmonic extraction algorithm is not required. Schematic of this scheme as shown in Fig.4. is briefed as follows. The difference of voltage of capacitor which is DC and its reference is given to the PI controller. When the output of the PI controller is multiplied with sinθ, the reference signal is generated.

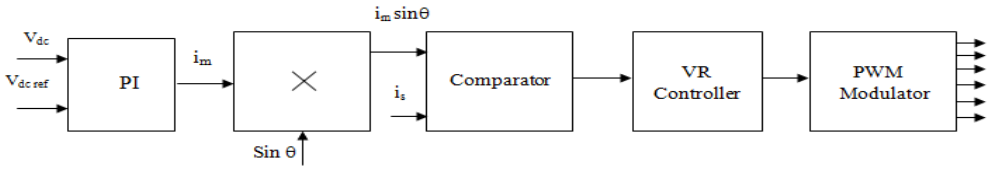

Figure 3: Block diagram of Power balance scheme

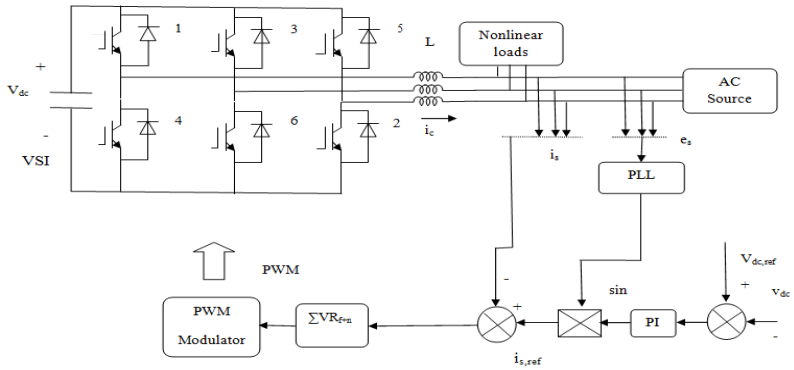

Figure 4: Configuration of Power balance scheme

Current Controller

A. Hysteresis current controller

The technique by which this controller is controlled, relies on the comparison of the actual phase current with the hysteresis band around the reference current of the same phase. The switching signals obtained from the comparison of the current error with the hysteresis band are given to the shunt APF for controlling their ON/OFF period to achieve the desired output. The devices in the Shunt APF switch ON/OFF based on the switching signals. The drawback of hysteresis current controller is its switching frequency that can be widely varied. They introduce switching noise in the power grid and make the power switch uncontrolled in applications involving high power.

The switches in the Shunt active power filter are ON and OFF by using the following logic,

1. If $i_{cr} < (i_{cr}$*- Hysteresis Band), then switch 1 is OFF and switch 4 is ON in the first leg
2. If $i_{cr} > (i_{cr}$*+ Hysteresis Band), then switch 1 is ON and switch 4 is OFF in the first leg

Similarly, the same logic is applicable for the other two phases.

B. PWM Controller

PWM controller is the common controller, which generates the switching signal by comparing the reference signal with the carrier wave. The type of reference signals generated in the control strategies like p-q, SRF, current source and the power balance scheme is analyzed. If the reference signal generated is fundamental current, then fundamental current and supply current is compared and the resultant error signal is given to the PWM controller. This error signal is compared with the triangular carrier wave and the switching signals obtained are given to the shunt APF. Similarly, if the reference signal generated is harmonic current, then harmonic current and filter current is compared and the resultant error signal is given to the PWM controller. The PWM controller compares this signal with the triangular carrier wave and the switching pattern obtained is given to the shunt APF to control the ON/OFF of the power electronic devices, to inject the compensating current for the cancellation of harmonic current.

C. Vector resonant controller

The VR controller, which has got excellent selectivity, is used in this scheme for selective harmonic compensation. The divergence between the fundamental load current and the actual load current obtained in the current source scheme and the divergence between the fundamental source current and the actual source current obtained in the power balance scheme are given as input to the VR controller. With the help of cascade VR controllers selective harmonic compensation can be made. The harmonic order which needs to be eliminated is selected and given to the VR controller. Since, fifth harmonic frequency is the predominant one, the only fifth harmonic is compensated in this paper. The expression of VR controller is,

$$VR_r(s) = k_{VRr}\frac{s\left(s+\frac{R_{acr}}{L_{acr}}\right)}{s^2+(n\omega_{er})^2} \tag{34}$$

Where k_{VRr} is the gain of the controller. L_{acr}, R_{acr} is the equivalent inductance and resistance of the L and n ω_{er} is the corresponding resonant frequency. Subscript n

represents the selected harmonic order. Fig.5 represents vector resonant controller, which is cascaded.

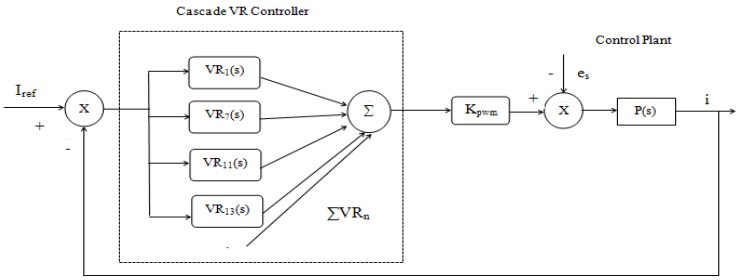

Figure 5: Cascade Vector Resonant Controller

Simulation Results

This section contains the outcomes of simulation studies carried out in MATLAB. Various simulation studies carried out are p-q theory with hysteresis controller, p-q theory with PWM controller, SRF with hysteresis controller, SRF with PWM controller. Fig.6 shows the simulink model of the simulation studies. Fig.7, Fig.8, Fig.9 and Fig.10 shows the load current, source current, FFT analysis of load and source currents obtained by p-q with hysteresis controller, Fig.11, Fig.12, Fig.13 and Fig.14 shows the load current, source current, FFT analysis of load and source currents obtained by p-q with PWM controller, Fig.15, Fig.16, Fig.17 and Fig.18 shows the load current, source current, FFT analysis of load and source currents obtained by SRF with hysteresis controller, Fig.19, Fig.20, Fig.21 and Fig.22 shows the load current, source current, FFT analysis of load and source currents obtained by SRF with PWM controller, Fig.23, Fig.24, Fig.25 and Fig.26 shows the load current, source current, FFT analysis of load and source currents obtained by current source scheme with VR controller, Fig.27, Fig.28, Fig.29 and Fig.30 shows the load current, source current, FFT analysis of load and source currents obtained by power balance scheme with VR controller.

Since, the nonlinear load used is 3ϕ diode bridge rectifier with R load in all the simulation studies, the load current waveform obtained is the same. The simulation results obtained has been verified using MATLAB/SIMULINK.

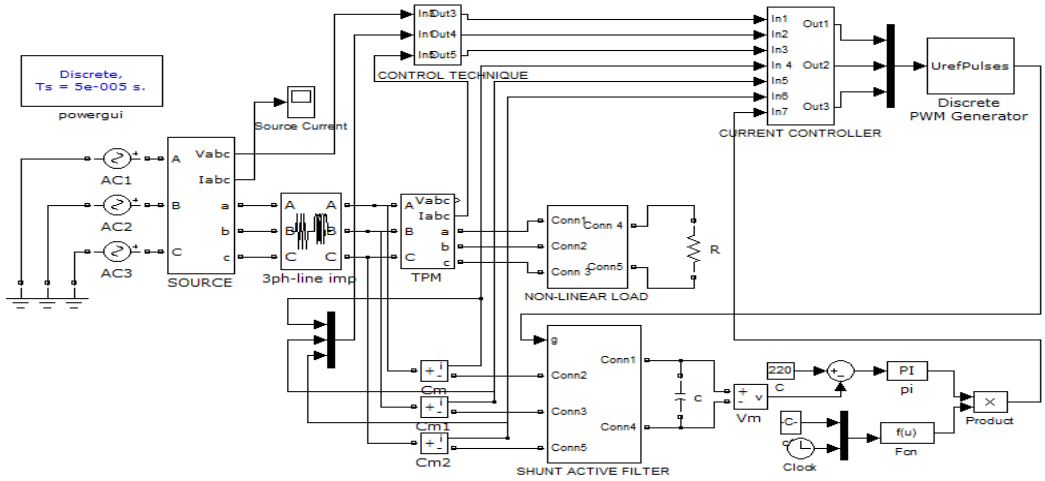

Figure 6: Simulink model of Reference current generation of SAPF using different algorithms

A. The simulation results of Simulink model employing p-q with Hysteresis controller

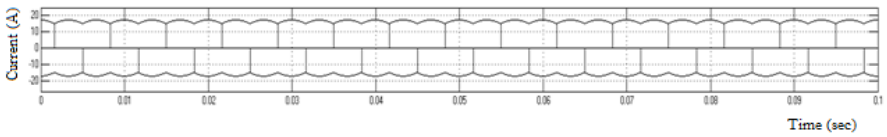

Figure 7: Output current waveform of 3ϕ diode bridge rectifier with R-load

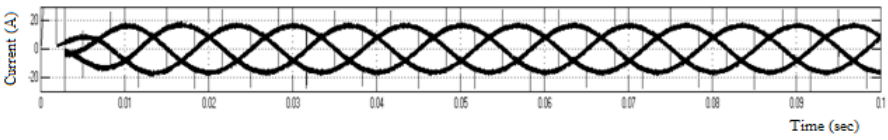

Figure 8: Source current waveform with filter

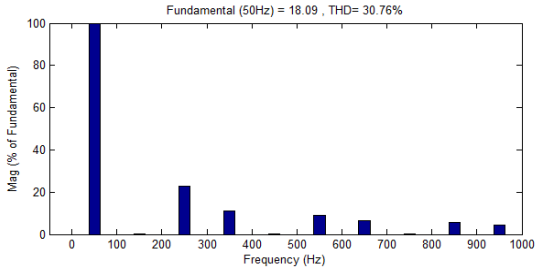

(R-Phase)

Figure 9: THD level of output current waveform (R-Phase)

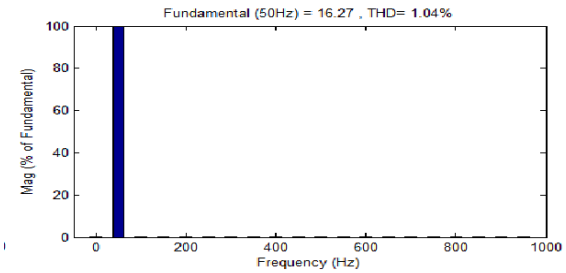

Figure 10: THD level of source current waveform with filter

B. The simulation results of Simulink model employing p-q with PWM controller

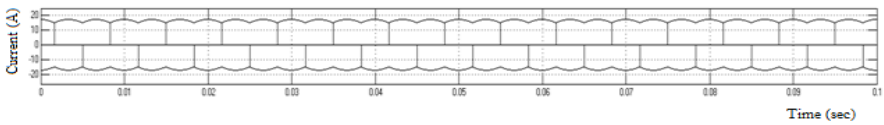

Figure 11: Output Current Waveform of 3ϕ Diode Bridge Rectifier With R-Load

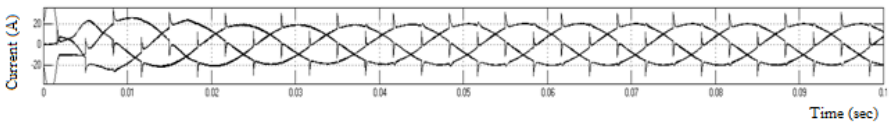

Figure 12: Source Current Waveform With Filter

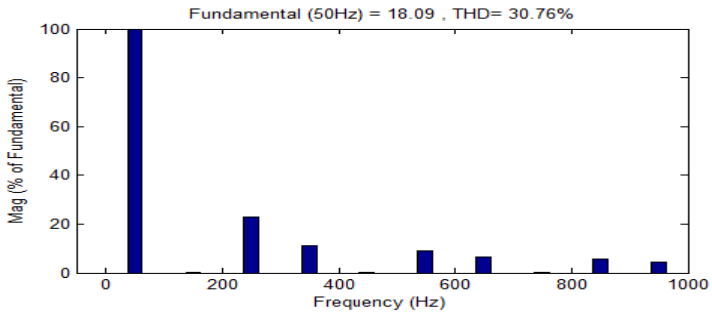

(R-Phase)

Figure 13: THD Level of Output Current Waveform (R-Phase)

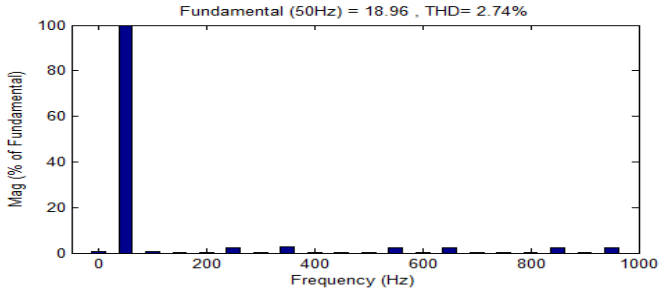

Figure 14: THD Level of Source Current Waveform With Filter

C. The simulation results of Simulink model employing SRF with Hysteresis controller

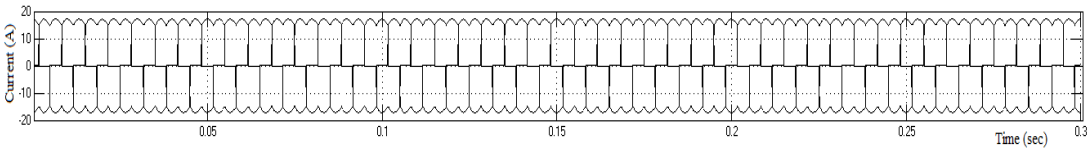

Figure 15: Output Current Waveform Of 3ϕ Diode Bridge Rectifier With R-Load

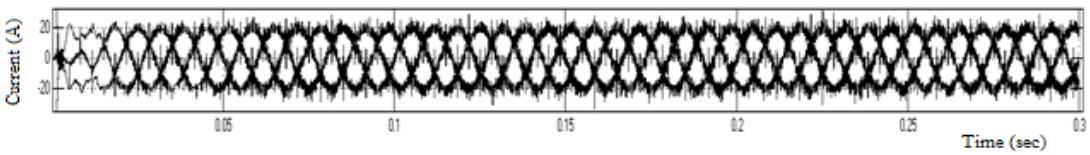

Figure 16: Source Current Waveform With Filter

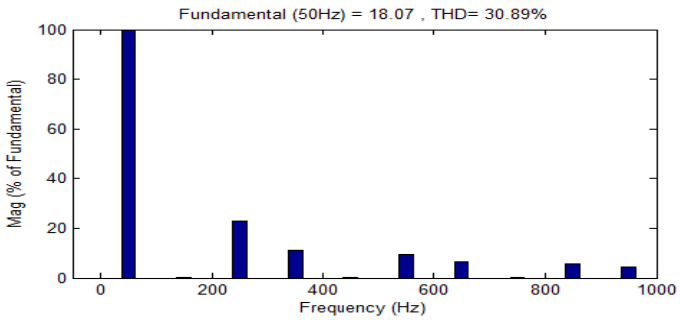

(R-Phase)

Figure 17: THD levels of output current waveform (R-Phase)

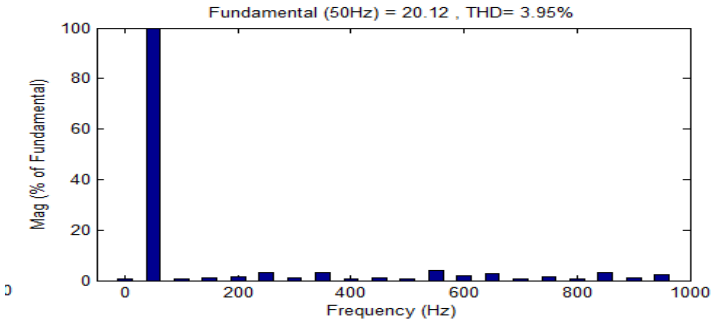

Figure 18: THD levels of source current waveform with filter

D. The simulation results of Simulink model employing SRF with PWM controller

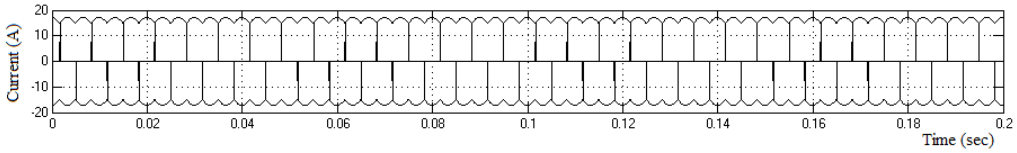

Figure 19: Output Current Waveform of 3ϕ Diode Bridge Rectifier With R-Load

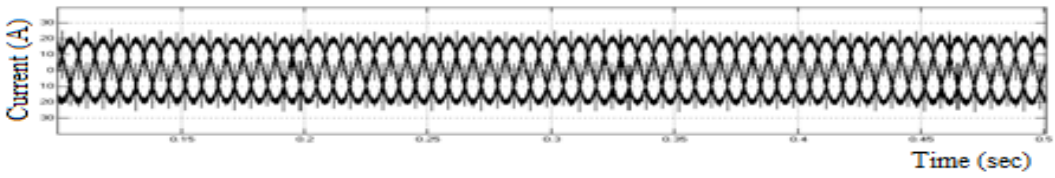

Figure 20: Source Current Waveform With Filter

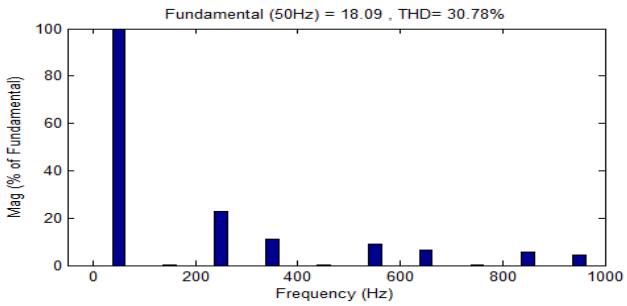

(R-Phase)

Figure 21: THD levels of output current waveform (R-Phase)

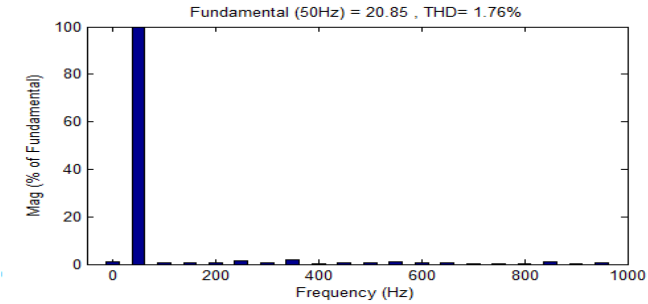

Figure 22: THD Levels of Source Current Waveform With Filter

E. The simulation results of Simulink model employing Current Source scheme with the Vector Resonant controller

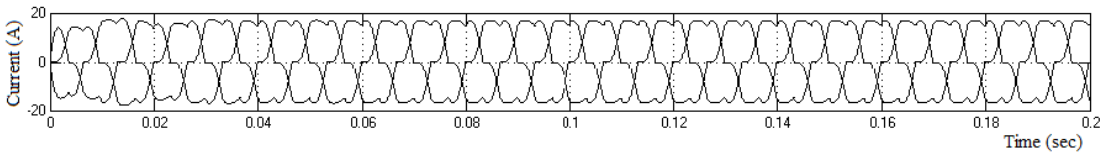

Figure 23: Output Current Waveform of 3ϕ Diode Bridge Rectifier With R-Load

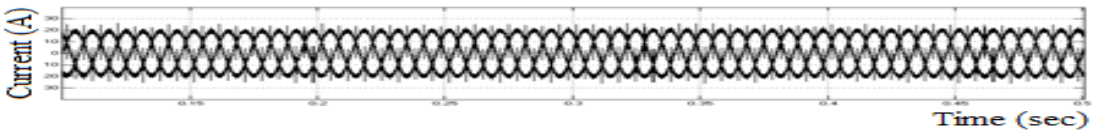

Figure 24: Source Current Waveform With Filter

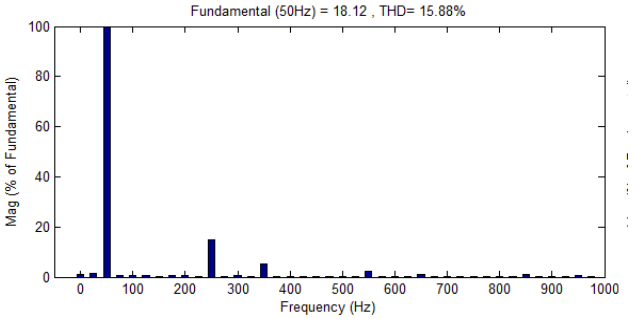

(R-Phase)

Figure 25: THD Levels of Output Current Waveform (R-Phase)

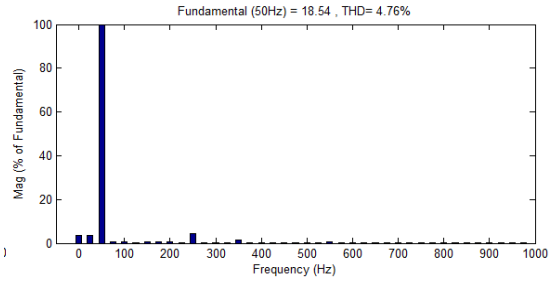

Figure 26: THD Levels of Source Current Waveform With Filter

F. The simulation results of Simulink model employing Power Balance scheme with the Vector Resonant controller

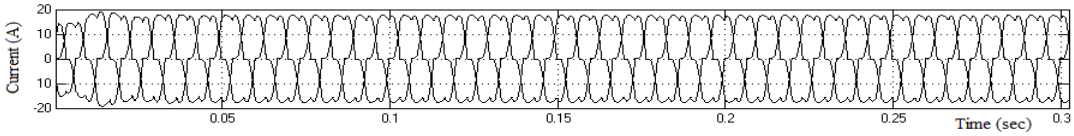

Figure 27: Output current waveform of 3ϕ diode bridge rectifier with R-load

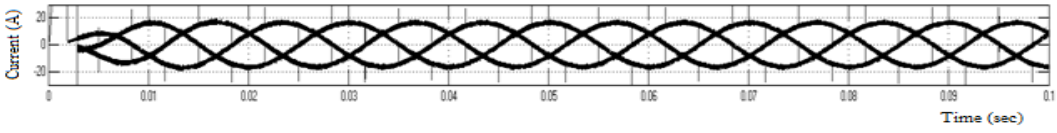

Figure 28: Source Current Waveform With Filter

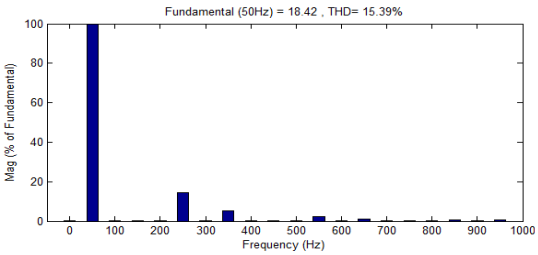

(R-Phase)

Figure 29: THD level of output current waveform (R-Phase)

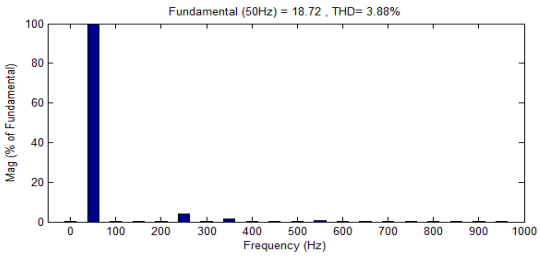

Figure 30: THD level of source current waveform with filter

From the simulation results, THD of source current has been reduced to, 1) 1.04% by employing p-q with Hysteresis controller, 2) 2.74% by employing p-q with PWM controller, 3) 3.95% by employing SRF with Hysteresis controller, 4) 1.76% by employing SRF with PWM controller, 5) 4.76% by employing CS scheme with VR controller, 6) 3.88% by employing PB scheme with VR controller. Thus the THD has been reduced to less than 5% in all the methods.

Conclusion

This paper proposes two control techniques and one current controller namely, Current Source scheme, Power Balance scheme and Vector Resonant controller. Current controller named Vector Resonant controller is preferred in this paper, because of its excellent selective harmonic compensation. From the comparative analysis carried out on simulation results, it is found that even though the PWM controller is quite complex when compared to the hysteresis controller, it has got a constant switching frequency that can be reasonably varied. Due to this reason, its switching losses are minimum when compared to hysteresis controller, which has got switching frequency that can be widely varied. Because of this reason, the advantage of PWM controller outweighs the advantages of Hysteresis controller. On comparing CS and PB scheme, PB scheme has got good harmonic filtering performance compared to CS scheme. This can be proved by the statistical data given above. In addition to this, harmonic extraction algorithm is not required in PB scheme. So, the computations involved in PB scheme are less when compared to CS scheme.

References

[1] Bimal K. Bose, "Modern Power Electronics and Drives", Prentice Hall PTR, 2002.

[2] R. Krishnan, "Electric Motor Drives-Modeling, Analysis and Control", second edition prentice-Hall of India Private Limited, New Delhi.

[3] Mohammad H. Rashid, "Power Electronics Handbook"- Devices, Circuits and Applications", Academic Press, 2001.

[4] W. Mack Grady and San Diego Gas & Electric, "Harmonics and how they relate to Power Factor" Proc. of the EPRI Power Quality Issues & Opportunities Conference (PQA'93), San Diego, CA, November 1993.

[5] R. Sriranjani, M. Geetha and S. Jayalalitha, "Harmonics and reactive power compensation using Shunt Hybrid filter", RJASET, 5(1) January 2013.

[6] R. Sriranjani and S. Jayalalitha, "Comparison of passive active and hybrid filter in front end system", IJCEA, vol 3, no.3, pp 503- 506, July 2012.

[7] R. Sriranjani and S. Jayalalitha, "LMS algorithm based fundamental current detection for Shunt hybrid filter", Journal of applied science, VOL 14, 14, PP. 1612-1617, 2014.

[8] R. Sriranjani and S. Jayalalitha, "Investigation of the performance of various types of filter", WASJ, vol 17, no.5, pp 643-650, 2012.

[9] S.H. Reyes, S. Patricio and K. Hyosung, "Instantaneous reactive power theory applied to active power filter compensation: Different approaches, assessment and experimental results," IEEE Trans. Ind. Electron., vol.55, no.1, pp. 184-196, Jan.2008.

[10] B. Geethalakshmi and M. Kavitha, "Comparison of Reference Current Extraction Methods for Shunt Active Power Filters" International Journal of Computer and Electrical Engineering, vol.3, No.3, June 2011.

[11] H. Akagi, Y. Kanazawa, A. Nabae, "Instantaneous Reactive Power Compensator Comprises Switching Device without Energy Storage Components", IEEE Trans. Ind. Applications 1984.

[12] R. Sriranjani and S. Jayalalitha, " Improvement of the time domain specifications of DC bus voltage of shunt active filter using controllers", IEEE International Conference on recent advancement in Electrical, Electronics and Control Engineering, Mepco Schlenk Engineering College, pp(187-191), 2011.(IEEE Explorer).

[13] Chennai Salim, Benchouia M-T, "Three-Phase Three-wire Shunt Active Power Filter Based on Hysteresis, Fuzzy & MLPNN Controllers to Compensate Current Harmonics " Journal of Electrical and Control Engineering Vol. 3 No. 3, 2013.

[14] C. Lascu, L. Asiminoaei, I. Boldea and F. Blaabjerg, "High performance current controller for selective harmonic compensation in active power filters", IEEE Trans. Power Electron., vol. 27, no. 5, pp. 1826-1835, Sep-2007.

[15] R. Venkatesh, S. Dinesh Kumar, R. Sriranjani and S. Jayalalitha, "Performance analysis of harmonic reduction by shunt active power filter using different control techniques" , Journal of Theoretical and Applied Information Technology, vol 63,1, PP 226 -232, 2014.